



Original Article

Optimizing the batch fermentation process (agitation and aeration) of the biocontrol agent, *Bacillus velezensis* strain KSAM1, and its influence on soilborne fungus, *Macrophomina phaseolina*

Abdulaziz Al-Askar^{a,*}, Fatimah Al-Otibi^a, Gaber A. Abo-Zaid^b, Ahmed Abdelkhalek^c

^aDepartment of Botany and Microbiology, College of Science, King Saud University, P.O. Box 2455, Riyadh 11451, Saudi Arabia

^bBioprocess Development Department, Genetic Engineering and Biotechnology Research Institute, City of Scientific Research and Technological Applications, New Borg El-Arab City, Alexandria 21934, Egypt

^cPlant Protection and Biomolecular Diagnosis Department, Arid Lands Cultivation Research Institute, City of Scientific Research and Technological Applications, New Borg El-Arab City, Alexandria 21934, Egypt

ARTICLE INFO

Keywords:

Bacillus velezensis
Batch fermentation
GC-MS
Macrophomina phaseolina
Optimization
Secondary metabolites

ABSTRACT

Macrophomina phaseolina is a soilborne fungus responsible for developing root-rot and charcoal-rot diseases in various plants. Seventeen *Bacillus* strains were isolated and assessed as potential biocontrol agents to determine their capability to suppress *M. phaseolina* growth. The KSAM1 isolate demonstrated the highest efficacy in suppressing fungal mycelial growth, achieving an inhibition rate of 38.6%. The 16S rRNA gene sequencing, BLAST analysis, and phylogenetic tree construction demonstrate that KSAM1 is *Bacillus velezensis*. It is registered in GenBank as *B. velezensis* strain KSAM1 (Acc# PQ288980). Subsequently, two batch fermentation processes were implemented in an agitated tank bioreactor to optimize agitation and aeration to achieve the highest possible level of culture biomass and secondary metabolite production. The maximum achievable level of the culture biomass was 3.92 g L⁻¹, which was achieved at 10.5 hours through the utilization of batch fermentation No. 2. This process involved stirring at rates between 200 and 600 rpm, along with an aeration rate of 1 VVM. This achievement was realized while upholding a steady specific growth rate (μ) of 0.08 h⁻¹. The observations indicated that the biomass yield coefficient was established at 0.7 g cells/g glucose. The analysis of bacterial filtrate extract using gas chromatography-mass spectrometry indicated that diisooctyl phthalate was the most bioactive secondary metabolite compound in the chromatogram, accounting for 36.07 percent of the total area. Overall, *B. velezensis* strain KSAM1 may serve as a biocontrol agent for *M. phaseolina*, as indicated by the results of the present investigation.

1. Introduction

Macrophomina phaseolina is a type of ascomycete that belongs to the family *Botryosphaeriaceae*. It is primarily found in soil and is widely dispersed in warm regions (Dhingra and Sinclair, 1978; Marquez et al., 2021). It causes root rot and charcoal rot diseases affecting over 500 species of both cultivated and wild plants (Sassenrath et al., 2024). Several of these diseases affect economically significant crops, including soybeans, sesame, sunflowers, maize, cotton sorghum, cowpea, and strawberries (Rangel-Montoya et al., 2022). One indication of *M. phaseolina* infection in plants is the decay of the stem and roots, accompanied by chlorotic foliage and leaf senescence (Salahlou et al., 2016). The fungus produces microsclerotia, which are resistant structures. These microsclerotia can persist in soil, agricultural residues, and seeds for a period ranging from 2 to 15 years. Furthermore, in the late stages of the disease, they can be found in the root and stem tissues (Meyer et al., 1974).

For more than seven decades, researchers have been investigating the possibility of employing specific bacteria as biocontrol agents to manage soilborne plant pathogens (Abdelkhalek et al., 2020; Abed

et al., 2016). This research has been conducted as a substitute or supplementary approach to controlling diseases using pesticides. Plant growth-promoting rhizobacteria (PGPR) significantly contribute to the improvement of plant growth by efficiently controlling phytopathogens. This contribution is significant for maintaining ecological balance and ensuring the sustainable future of agriculture. To exert control over the growth of phytopathogens, PGPR employs a range of antagonistic activities. Some of these processes include making antibiotics, cellulolytic enzymes, hydrolytic enzymes, organic volatile chemicals, extracellular antifungal metabolites, and cyanides (Maral-Gül and Eltem, 2024). Beneficial strains of *Bacillus* are widely recognized for their application in biological control (Fendrihan et al., 2016). These strains are also considered to be important prospects for PGPR. Over the past century, *Bacillus* bacteria have been employed as biological control agents because of their ability to endure in the rhizosphere and reduce the emergence and progression of plant diseases. Furthermore, these bacteria's ability to produce endospores gives them a degree of climatic tolerance, which is crucial for the formation of inoculum (Sabaté et al., 2020; Torres et al., 2017). Various *Bacillus* species have been utilized due to their promising uses as microbial biopesticides (Kiesewalter et al., 2021).

*Corresponding author:

E-mail address: aalaskara@ksu.edu.sa (A. Al-Askar).

Received: 2 October, 2024 Accepted: 5 January, 2025 Epub Ahead of Print: 28 February, 2025 Published: 22 March, 2025

DOI: 10.25259/JKSUS_117_2024

Stirred-tank bioreactors are commonly used to increase the scale of microbial production processes. This is because bioreactors provide superior control and optimization environments. The up-scaling procedure begins with cultivation in laboratory bioreactors. The next step involves cultivating bioreactors of varying sizes, ranging from semi-pilot to pilot, and ultimately, the process is carried out in tanks designed for mass production (Connors, 2003). The environment within the bioreactors promotes a more consistent and optimal setting for cell growth due to the rapid and uniform stirring and mixing, along with the minimal fluctuations in hydrostatic pressures within the vessel (Jahanian et al., 2024). To optimize biomass and secondary metabolite production, it is essential to analyze and refine numerous operational parameters. These parameters include agitation, aeration, and dissolved oxygen concentration. The key process parameters are agitation and aeration, as both significantly affect the oxygen transfer to the cells, which is essential for scaling up aerobic fermentation (Zhou et al., 2018). The solubility of oxygen and diffusion into the broth are both associated with the process of oxygen transfer (Caçaval et al., 2011). There is a significant enhancement in both the progression and production kinetics that occurs when production systems are scaled up from the shake-flask level to the bioreactor level. This is primarily because it provides developing cells with improved environmental conditions, namely oxygenation, aeration, agitation, and mixing dynamics (Elsayed et al., 2019).

The current study aims to explore the inhibitory effects of seventeen different *Bacillus* isolates regarding their potential application as biocontrol agents against *M. phaseolina*, which is responsible for root-rot and charcoal-rot diseases. Utilizing 16S rRNA to determine the identity of the *Bacillus* isolate KSAM1 is the next step in the process. Furthermore, two batch fermentation processes were conducted in a stirred tank bioreactor to refine the parameters of agitation and aeration, aiming to enhance the yield of KSAM1 biomass and secondary metabolites. The final step involved utilizing GC-MS to analyze the secondary metabolites extracted from the culture filtrate.

2. Materials and methods

2.1 Experimental isolation procedures

Using soil dilution from the rhizospheres of tomato, potato, eggplant, and pepper, isolation studies were carried out in the Kingdom of Saudi Arabia (KSA). One gram of soil was stirred for fourteen minutes in a sterile saline solution with 0.85% NaCl. Dilutions of the 10^{-5} , 10^{-6} , and 10^{-7} were made and 200 μ L of each were disseminated onto glycerol nutrient agar and peptone nutrient agar media. Many bacterial colonies were evident after 48 hours of incubation at 30 °C. The technique of isolating a single colony facilitated the separation and refinement of the identified colonies. The bacterial cultures were kept in 50% glycerol broth at -80 °C for future studies. The isolate of *M. phaseolina* was graciously supplied by the Plant Protection Department at the City of Scientific Research and Technological Applications in Egypt.

2.2 *Bacillus* isolates antagonism test

A laboratory antagonist assay was performed to assess the effectiveness of *Bacillus* isolates as biocontrol agents targeting the plant pathogenic fungus *M. phaseolina*. A loop-full of a two-day-old culture was used to spread the antagonistic bacterial isolates along a streak line on petri dish plates enriched with potato dextrose agar (PDA) medium. The plates were then left to grow for 48 hours before any tested fungus was added. A 5 mm mycelial disc from a rapidly growing culture was used to place the fungus under study in the middle of the petri dish, a fixed distance from the other edge. The dish was then kept at 30°C for 3 to 7 days. The fungal growth inhibition percentage was assessed by calculating the reduction in growth of the tested fungus in the presence of the antagonistic bacteria, as previously outlined (Maurhofer et al., 1995). Each experiment was conducted with three repetitions for every fungus. The results were analyzed using a complete randomized design (CRD) through one-way ANOVA. The least significant difference (L.S.D.) test was performed using the CoSTAT program (version 6.311, 2005, USA) at a significance level of 0.05.

2.3 Molecular characterization of the hopeful *Bacillus* isolate

One pure colony of strain KSAM1 was added to 5 mL of Luria-Bertani broth medium. The inoculated medium was mixed and incubated at 30°C overnight. Total DNA was extracted from a 1 mL bacterial pellet using an extraction and purification kit (Promega, USA). The purity and integrity of isolated DNA were assessed through agarose gel electrophoresis, and its concentration was measured with the NanoDrop ND-1000 spectrophotometer. The concentration of DNA was adjusted to 50 ng/ μ L before being used in the polymerase chain reaction (PCR) reaction. Specific universal primers (F: AGAGTGATCCTGGCTCAG, R: GGTTACCTGTGTTACGACTT) were utilized to amplify the 16S rRNA gene. The 20 μ L PCR reaction included 10 μ L of PCR master mix, 1 μ L of each primer (10 pM/ μ L), 1 μ L of template DNA (50 ng/ μ L), and 7 μ L of mill-Q double distilled water. The PCR thermal profile began with initial denaturation at 94°C for 4 minutes, followed by 35 cycles that included denaturation at 94°C for 50 seconds, annealing at 50°C for 50 seconds, and extension at 72°C for 90 seconds, finishing with a final extension at 72°C for 5 minutes. (Yassin et al., 2024). After that, methods for purification and sequencing (Sanger technique) were used on the PCR fragments. As soon as the sequences with explanations were added to GenBank, they were compared to isolates that had already been published. Twenty thousand bootstrap replications were executed to generate the phylogenetic tree. The UPGMA algorithm was employed alongside MEGA software version 11 to achieve this.

2.4 Experiment on fermentation

2.4.1 Bioreactor (fermentor)

The *B. velezensis* strain KSAM1, demonstrating significant potential, was cultivated and fermented in a ten-liter benchtop bioreactor (Cleaver, Saratoga, USA), including four baffles and two turbine impellers with six-bladed discs. A computerized control system was utilized to oversee the batch fermentation process with a capacity of four liters. An automated process was managed via a device featuring a 10.4-inch color touch-screen interface. This gadget can store up to 59,994 unique programs for different scenarios. The batch fermentation process was executed at 30°C and a pH of 7, which was meticulously regulated. A standard solution of 2N NaOH and 2N HCl was automatically provided for pH adjustment. After the air was filtered through a sterile filter, it was compressed and calibrated with a flowmeter to a flow rate of 0.5-1 VVM. The agitation speed was first established at 200 rpm and subsequently adjusted manually (200–600 rpm) to ensure that the dissolved oxygen concentration remained above 20%. The assessment of dissolved oxygen content and pH levels was conducted using METTLER TOLEDO electrodes (Moustafa et al., 2009).

2.4.2 Batch fermentation process

A single colony of the promising *B. velezensis* isolate KSAM1 was introduced into a 0.5 L Erlenmeyer flask containing 0.1 L of number 3 medium (production medium), which comprised 1 g of glucose, 1 g of peptone, 0.05 g of MgSO₄ · 7H₂O, and 0.1 g of KH₂PO₄ (Asaka and Shoda, 1996). Subsequently, the cell broth was allowed to incubate overnight at 30 °C while maintaining constant agitation at a speed of 200 rpm. The stirred tank bioreactor was used for performing two separate batches of fermentation. The aeration rate for batch No. 1 was set at 0.5 VVM, with agitation speeds fluctuating between 200 and 350 rpm. In contrast, batch No. 2 had an aeration rate of 1 VVM, and the agitation speed spanned from 200 to 600 rpm. A stirred tank bioreactor was used with a working capacity of 4 liters to start the batch fermentation process at an optical density (OD₅₅₀) of 0.5. Culture samples were collected during the fermentation process to measure the concentration of biomass and glucose.

2.4.3 Analytical methods

2.4.3.1 Assessment of cell biomass

As part of the cell count monitoring process, a spectrophotometer was used to measure the optical density (OD) of the culture at 550

nm. After centrifuging a sample of 10 mL with a force of 894 g for 10 minutes, the cell mass was reinstated, purified, and then subjected to centrifugation once more in order to determine the cell weight. This process was repeated multiple times. Subsequently, the pellet underwent a drying procedure that continued throughout the night in a dry-air oven at 80°C, as previously outlined (Van Dam-Mieras et al., 1992)

2.4.3.2 Measurement of glucose concentration

A colorimetric kit utilizing enzymatic methods (Diamond Diagnostics, Egypt) was used to determine the glucose content. This methodology depends on peroxidase and glucose oxidase. The quinoneimine dye, utilized as a glucose concentration indicator, converts into a reddish-violet hue as the final product.

2.5 GC-MS analysis

The bioactive constituents of the beneficial *B. velezensis* isolate KSAM1 were identified using GC-MS analysis. To do this, ethyl acetate was added to the culture filtrate, which was obtained by centrifugation of the culture broth, in a volume ratio of 1:1. After 10 minutes of vigorous stirring and 5 minutes of sitting, two separate layers formed, which did not mix, as reported previously (Hirpara et al., 2016). A separation funnel was employed to distinguish the different layers of the solvent. The extracted biomolecules were in the upper layer (ethyl acetate phase). As previously reported, we further concentrated the ethyl acetate extract by evaporating the solvent in a rotary evaporator while maintaining vacuum (Sharma et al., 2016). Once the ethyl acetate had evaporated, brown gum became visible. It was kept at 4°C to preserve the crude extract. The GC-MS analysis of the generated residues was carried out using an Agilent 7000D instrument (Santa Clara, California, United States), with the program conditions set following the protocol described previously (Khamis et al., 2023).

3. Results

3.1 Isolation of *Bacillus* isolates

Bacillus isolates were isolated from the rhizospheres of tomato, potato, eggplant, and pepper during an isolation experiment conducted in the Kingdom of Saudi Arabia. During this investigation, 17 different *Bacilli* were isolated. *Bacillus* isolates BM1, BM2, and BM3 were initially a part of group 1, which was isolated from the tomato plant's rhizosphere. Separated from the potato rhizosphere was group 2, which included BM6, BM7, BM10, BM11, BM12, and BM13. Additionally, group 3 was responsible for the isolation of BM14, BM15, BM16, and BM17 from the rhizosphere of the eggplant. Finally, group 4 included *Bacillus* isolates of BM18, BM19, BM20, and BM21, which were isolated from the rhizosphere of the pepper plant.

3.2 Antagonism test of *Bacillus* isolates

Seventeen different *Bacillus* isolates were tested in vitro to see whether they had the capacity to limit the growth of *M. phaseolina*. The purpose of this investigation was to establish whether these isolates might be potential biological control agents. It was established that there were considerable differences between the *Bacillus* isolates, and this was because they exhibited antagonistic activity against *M. phaseolina*. It was discovered that the BM1 isolate was more effective than others in suppressing the development of *M. phaseolin*-generated fungal mycelia. Furthermore, it exhibited the highest percentage of inhibition against the pathogen, which reached 38.6%. This was followed by *Bacillus* isolate BM6, which recorded an inhibition percentage of 34.1%. *Bacillus* isolates BM2, BM7, BM10, and BM11, which did not exhibit any significant differences amongst themselves, demonstrated antagonistic activity against *M. phaseolina* that reached 28.6%, 28.2%, 26.7%, and 28.6%, respectively. On the other hand, *Bacillus* isolates BM13, BM17, BM18, and BM21 did not exhibit any antagonistic action against the fungal pathogen (Fig. 1).

3.3 Molecular characterization of the hopeful *Bacillus* isolate

Based on the phylogenetic tree analysis and the NCBI-BLAST alignment, the BM1 isolate was determined to be *B. velezensis* with the accession number PQ288980. The BLAST analysis indicated that the annotated sequence of the 16S rRNA gene of *B. velezensis* strain KSAM1 exhibited complete sequence coverage at 100% and a similarity identity of 99.65% with Chinese strains, particularly *B. velezensis* strain WW-61 (OM914855) and P66 (MZ396950). The annotated 1445 base pair nucleotide sequence has been uploaded to the GenBank database under the *B. velezensis* strain KSAM1 classification. Through the utilization of the 16S rRNA nucleotide sequences, a phylogenetic tree was constructed for the *B. velezensis* strain KSAM1 that was obtained in the current study and additional *Bacillus* species that were deposited in GenBank. Based on the phylogenetic tree, it was determined that there were two major clusters. The first cluster is subdivided into two groups. *B. velezensis* strain KSAM1 (PQ288980), which was obtained for this investigation, and some GenBank strains of the same species were grouped into the first group. The second group of the first cluster included other *Bacillus* species that were deposited in the GenBank database (Fig. 2).

3.4 Fermentation experiments

The batch fermentation number one of *B. velezensis* strain KSAM1 was conducted in a stirred tank bioreactor with a stirring speed between 200 and 350 rpm and an aeration rate of 0.5 VVM. It was observed that this strain exhibited a greater inhibition against the plant pathogenic fungus known as *M. phaseolina*. For the batch fermentation of *B. velezensis* culture broth, a plot was created that showed the concentration of biomass and glucose versus the time that had passed (Fig. 3a). After nine hours, the maximum amount of biomass was observed at 1.66 g L⁻¹. During the exponential stage, the logarithmic relationship was applied to obtain the constant specific growth rate (μ) of 0.17 h⁻¹. This resulted in an exponential increase in cell mass over time, as depicted in Fig. 3b. The biomass's natural logarithm (ln), which was calculated throughout the log phase, is depicted in the graph that originated before it as a linear path on a semi-logarithm that illustrates the relationship between time and biomass. The glucose concentration declined rapidly, reaching 0.98 g L⁻¹ after 6 hours and full consumption (0 g L⁻¹) at 11 hours (Fig. 3a). The biomass yield coefficient, also known as $Y_{x/s}$, is an important metric that is evaluated during the exponential stage of bacterial cell growth. This coefficient compares the amount of biomass that is achieved with the amount of glucose that is consumed as a carbon source. 0.37 grams of cells per gram of glucose was the biomass yield coefficient that was achieved by this batch fermentation process (Fig. 3c). During the exponential phase, additional factors were also measured to determine the effectiveness of the batch fermentation method's bacterial culture development process. Some aspects were taken into consideration, including the rate of cell mass creation (Q_x) and the rate of carbon supply consumption (glucose) (Q_s). As shown in Fig. 4, the rate of glucose intake (Q_s) was 0.24 g L⁻¹ h⁻¹, while the rate of biomass synthesis (Q_x) was 0.18 g L⁻¹ h⁻¹. The levels of dissolved oxygen (DO) influence the growth of bacterial cells. This concentration is influenced by the aeration rate and the agitation speed. For batch fermentation, we set the aeration rate to 0.5 VVM, the agitation speed to 200 rpm, and the level of dissolved oxygen to 97.4%. During the initial three hours, a steady decline in dissolved oxygen levels was observed, culminating in a 20% concentration at 2.4 hours. It is believed that a decrease in the amount of DO is a sign that the bacterial culture is developing and consuming the glucose that is present in the culture broth throughout the growth process. It was possible to keep the oxygen level at or above 20% by adjusting the speed of the agitation, which increased gradually from 200 to 350 rpm. The DO reached 40.3% at 7.6 hours and then gradually increased to 100% at 9 hours, a trend that continued until the end of the fermentation process. As a result, the agitation speed was decreased gradually, stage by stage, to reach 250 rpm (Fig. 5). The kinetic characteristics of batch fermentation No. 1 are detailed in Table 1.

For batch fermentation No. 2 of *B. velezensis* culture broth that was performed at agitation speed ranging from 200 to 600 rpm and an aeration rate of 1 VVM, a plot was created that showed the concentration

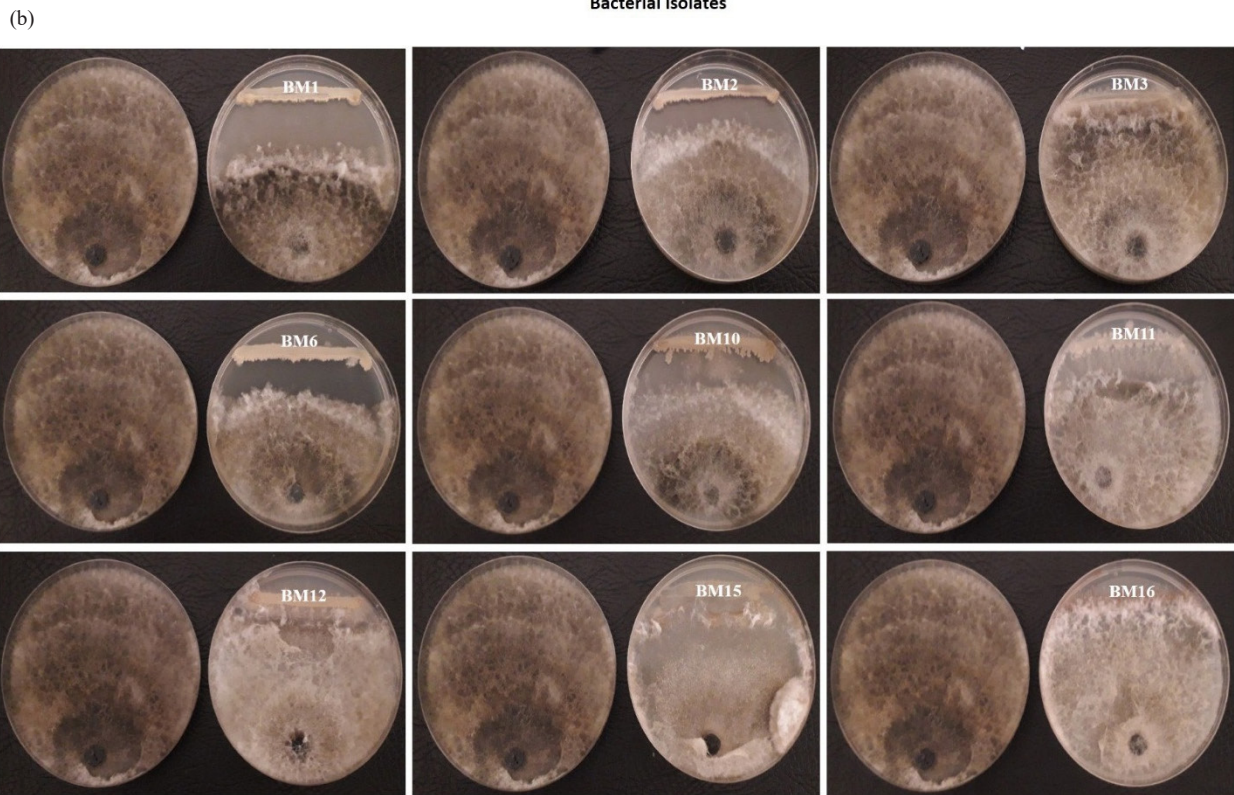
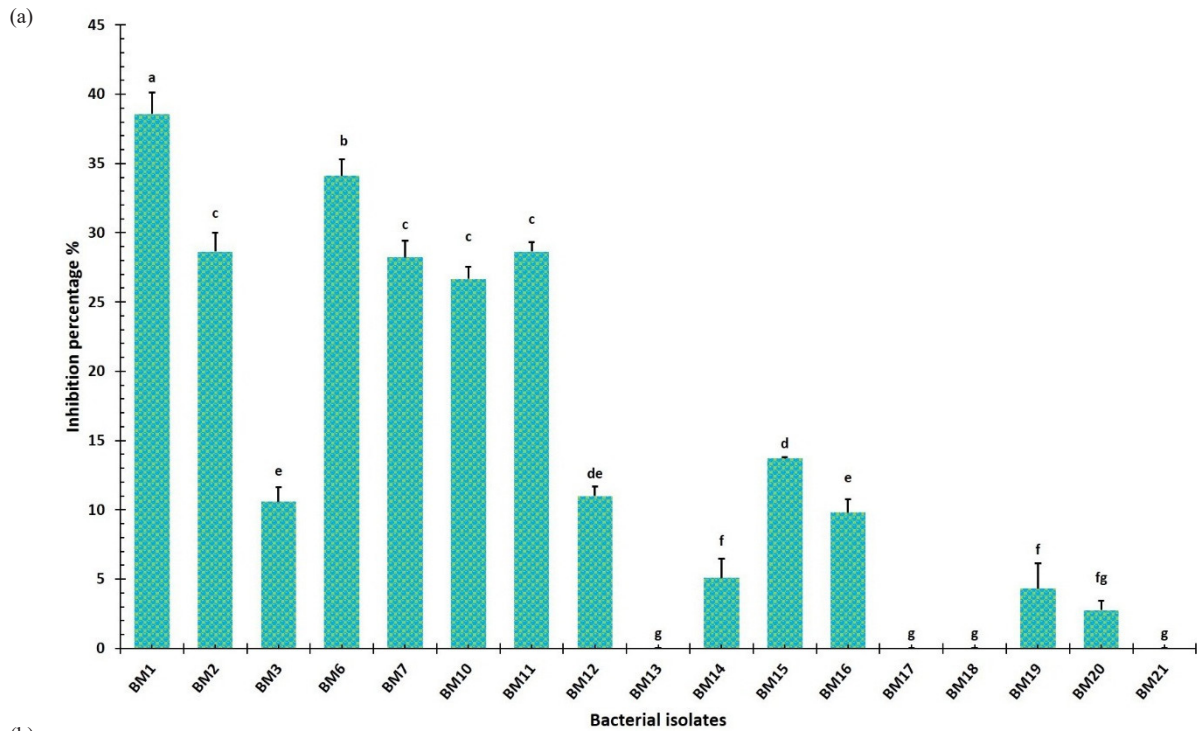


Fig. 1. (a) *Bacillus* isolates' percentage of inhibition against *Macrophomina phaseolina*, and (b) *Bacillus* isolates' antagonistic effects against *Macrophomina phaseolina*. The comparable fungus control on the left plate is free of antagonistic bacteria, while the fungus containing antagonistic bacteria is present on the right plate. The obtained results were analyzed using complete randomized design (CRD) through a one-way ANOVA. The least significant difference (L.S.D.) test was calculated at $p \leq 0.05$ of significance by CoSTAT software. Means on each column followed by the same lowercase letter do not differ significantly.

of biomass and glucose versus the time that had passed (Fig. 6a). After 10.5 hours, the maximum amount of biomass was observed at 3.92 g L⁻¹. During the exponential stage, the logarithmic relationship was applied to obtain the constant specific growth rate (μ) of 0.08 h⁻¹. This led to a significant growth in cell mass overtime, as depicted in Fig. 6b. The glucose concentration declined rapidly, reaching 0.54 g L⁻¹ after 6 hours, and completing consumption (0 g L⁻¹) at 7 hours (Fig. 6a). During

batch fermentation, the yield coefficient achieved was 0.7 g of cells per gram of glucose, in contrast to batch No. 1, which recorded 0.37 g cells/g glucose (Fig. 6c). Fig. 7 illustrates that the glucose consumption rate (Q_g) was measured at 0.96 g L⁻¹ h⁻¹, whereas the biomass synthesis rate (Q_x) was recorded at 0.49 g L⁻¹ h⁻¹. We started the batch fermentation with an agitation speed of 200 rpm, a rate of aeration equal to 1 VVM, and a higher value of DO equal to 99.5%. In the initial

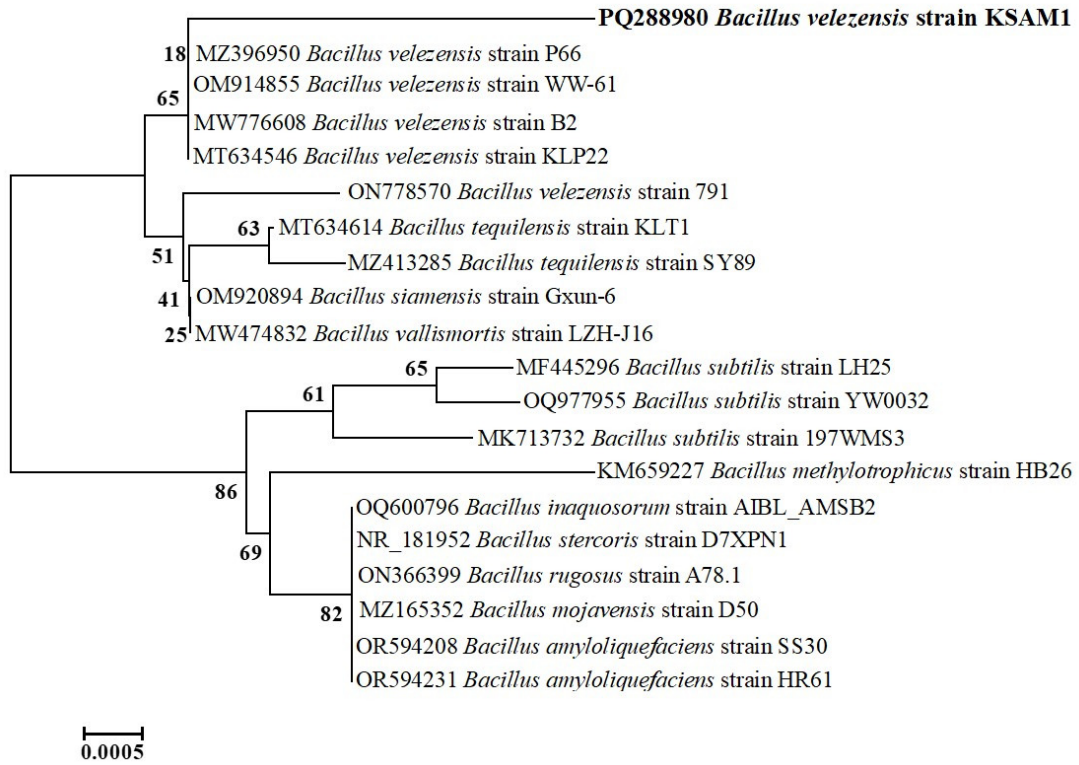


Fig. 2. UPGMA phylogenetic tree constructed using nearly complete 16S rRNA gene sequences of *B. velezensis* strain KSAM1 alongside other related strains sourced from Genbank. A total of 2000 bootstrap replications were conducted, and the phylogenetic tree was constructed utilizing MEGA version 11. UPGMA: Unweighted pair group method with arithmetic mean.

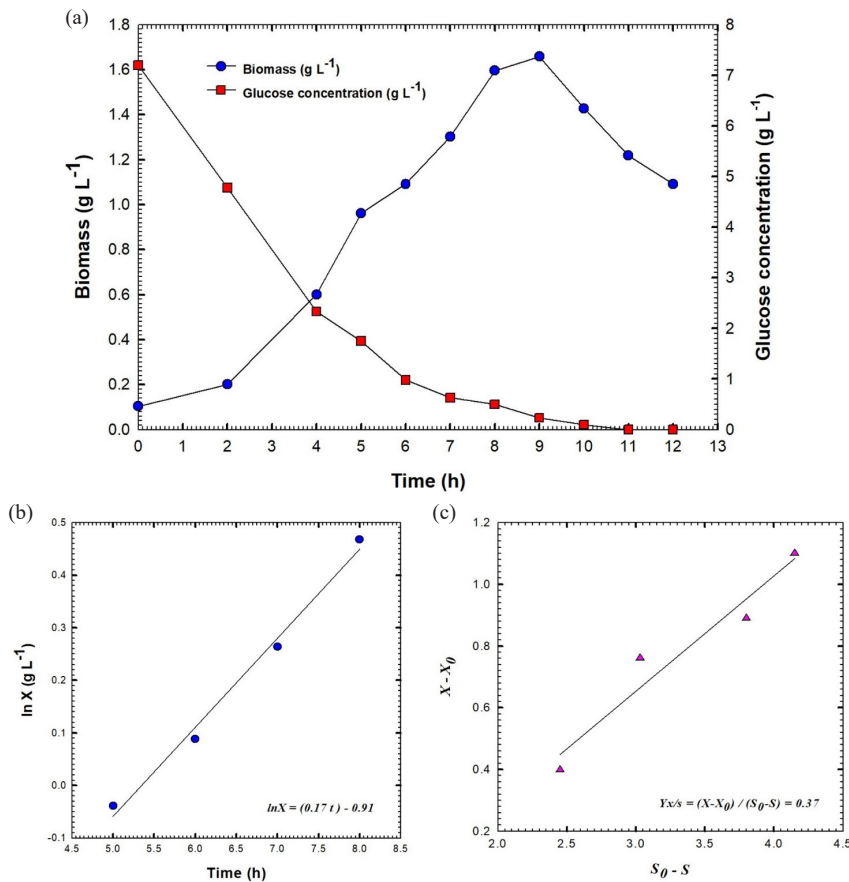


Fig. 3. (a) Shows the fermentation broth's glucose content and biomass against the time of batch fermentation No.1 of culture broth of *Bacillus velezensis* isolate KSAM1, (b) Shows the relationship between Ln biomass (X) and time and (c) Yield coefficient of biomass, $Y_{x/s}$, X_0 , X_t represent the culture biomass at primary time t_0 ; X_t , the culture biomass at time t ; S_0 , content of glucose in the culture at primary time t_0 and S_t , content of glucose in the culture at time t .

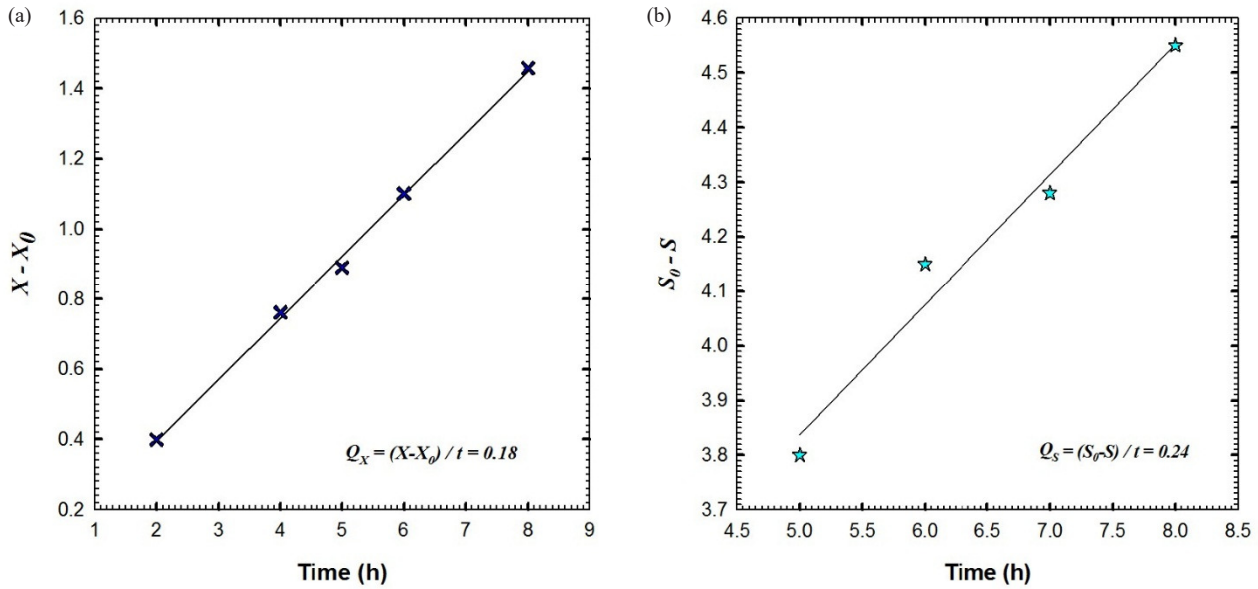


Fig. 4. (a) The rate of cell mass production (Q_x) and (b) the rate of glucose consumption (Q_s) as the substrate of batch fermentation No.1 of *Bacillus velezensis* isolate KSAM1.

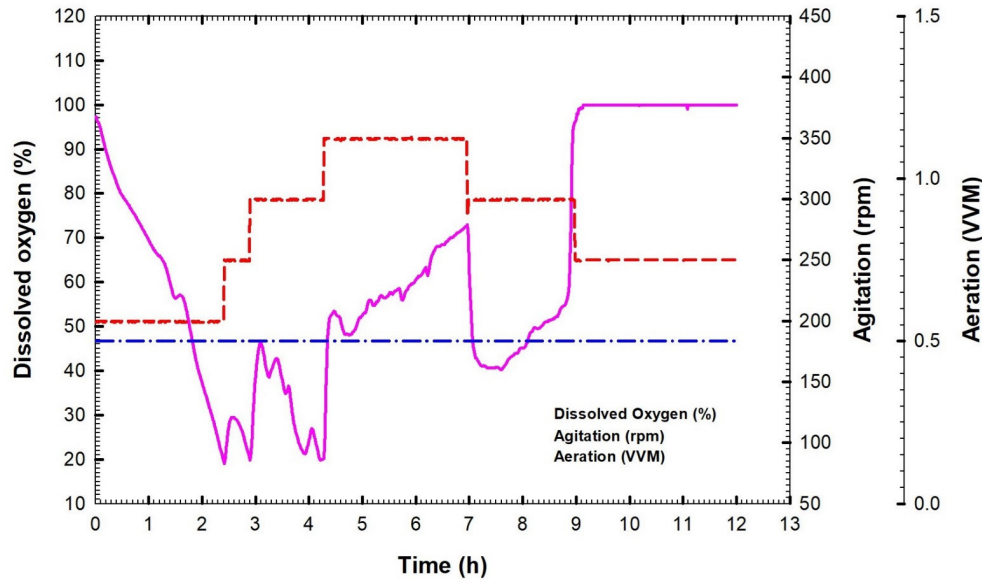


Fig. 5. The time-dependent dissolved oxygen, agitation, and aeration during *Bacillus velezensis* isolate KSAM1 batch fermentation No.1.

Table 1.

Kinetic parameters of *Bacillus velezensis* strain KSAM1 under different batch fermentation processes.

Kinetics parameters	Batch fermentation no. 1	Batch fermentation no. 2
$^* \mu$ (h^{-1})	0.17	0.08
$Y_{x/s}$ ($g\ g^{-1}$)	0.37	0.7
Q_s ($g\ L^{-1}\ h^{-1}$)	0.24	0.96
Q_x ($g\ L^{-1}\ h^{-1}$)	0.18	0.49
Overall cultivation time (h)	12 h	12 h

$^* \mu$ (h^{-1}), specific growth rate; $Y_{x/s}$ ($g\ g^{-1}$), yield coefficient of biomass; Q_s ($g\ L^{-1}\ h^{-1}$), consumption rate of glucose and Q_x ($g\ L^{-1}\ h^{-1}$), production rate of biomass.

two hours of batch fermentation, the concentration of dissolved oxygen gradually diminished, reaching 20% at the two-hour mark. The oxygen level was maintained at or above 20% by progressively increasing the agitation speed from 200 to 600 rpm to ensure that the dissolved oxygen remained above 20% (Fig. 8). Following two hours of culture growth, there was a rapid decline in the dissolved oxygen levels, while

the agitation speed steadily rose to 600 rpm. The agitation speed was systematically elevated in increments of 50 rpm, progressing from 200 rpm to 600 rpm. The agitation speed was increased in response to the oxygen demand, as follows: 250 rpm at 2 h, 300 rpm at 2.46 h, 350 at 4.9 h, 400 rpm at 7.13, 450 rpm at 7.81 h, 500 rpm at 8.03 h, 550 rpm at 8.76 h, and 600 rpm at 8.85 h. DO concentration decreased rapidly after 8.85 h, reaching 14% at 10.33 h, although the agitation speed increased by 600 rpm. After that, DO increased gradually to reach 80.2% at the end of the fermentation process. The kinetic parameters of batch fermentation No. 2 are presented in Table 1.

3.5 Identification of bioactive metabolites of *Bacillus velezensis*

The GC-MS analysis of the KSAM1 culture filtrate extract was used to find the specific compounds that might be responsible for their ability to fight *M. phaseolina* (Fig. 9). The GC-MS profile showed the existence of twenty-one different compounds in the culture filtrate of KSAM1 (Table 2). These compounds including diisooctyl phthalate (36.07%), tris(2,4-di-tert-butylphenyl) phosphate (22.82%), dibutyl phthalate

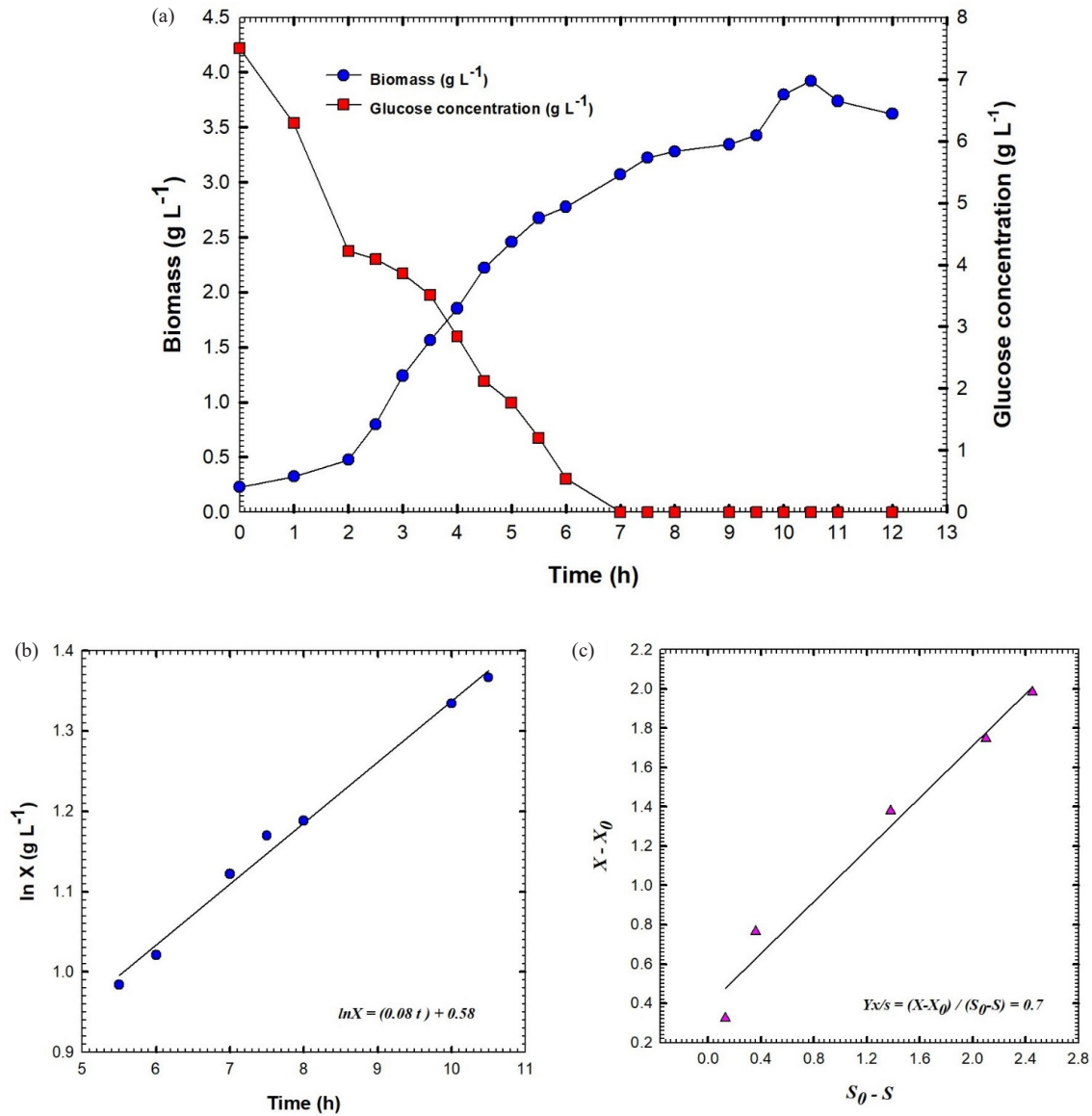


Fig. 6. (a) Shows the fermentation broth's glucose content and biomass against the time of batch fermentation No.2 of culture broth of *Bacillus velezensis* isolate KSAMI1, (b) Shows the relationship between Ln biomass (X) and time and (c) Yield coefficient of biomass, $Y_{x/s}$, X_0 , represent the culture biomass at primary time t_0 ; X, the culture biomass at time t; S_0 , content of glucose in the culture at primary time t_0 and S, content of glucose in the culture at time t.

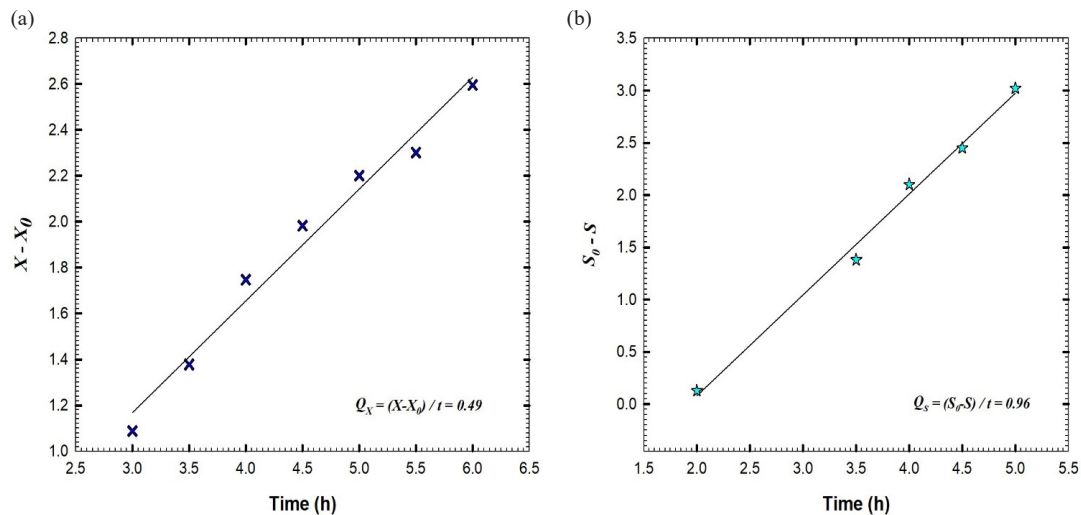


Fig. 7. (a) The rate of cell mass production (Q_x) and (b) the rate of glucose consumption (Q_s) as the substrate of batch fermentation No. 2 of *Bacillus velezensis* isolate KSAMI1.

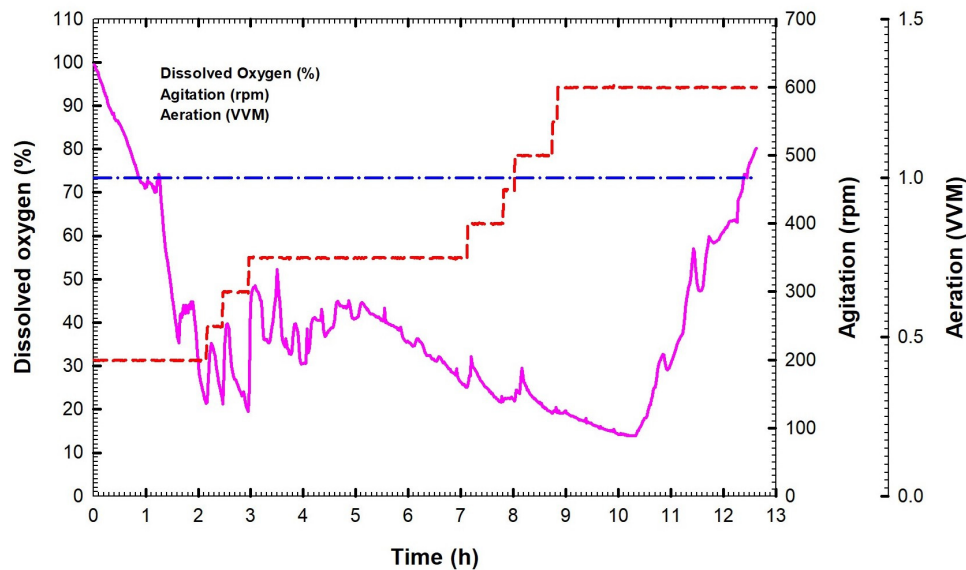


Fig. 8. The time-dependent dissolved oxygen, agitation, and aeration during *Bacillus velezensis* isolate KSAM1 batch fermentation No. 2.

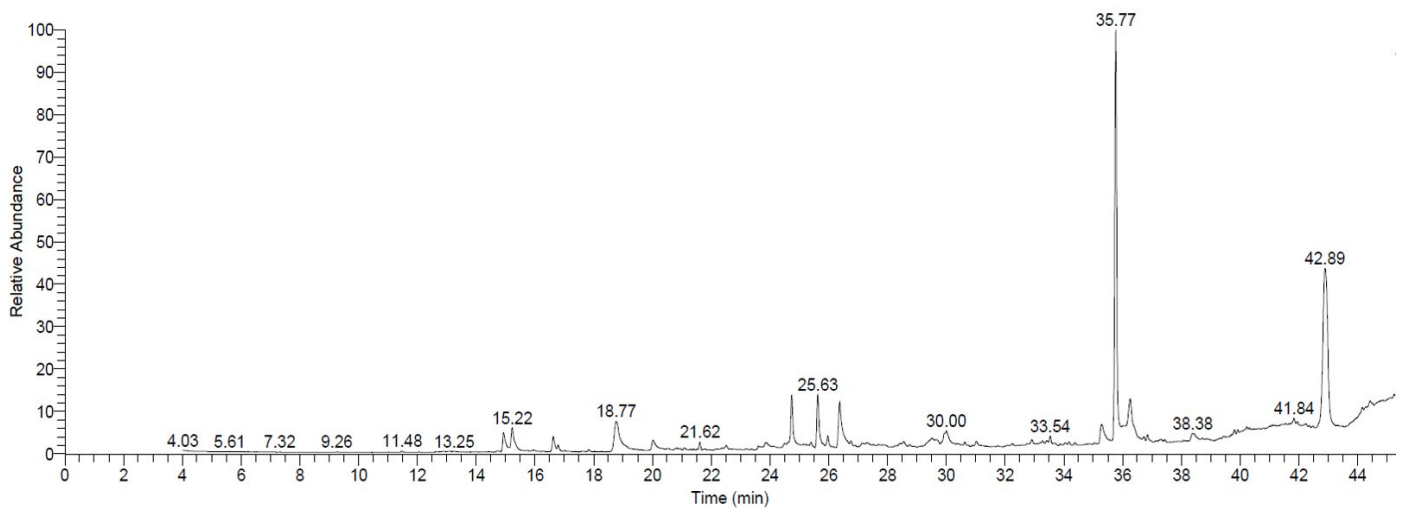


Fig. 9. GC-MS chromatogram of the ethyl acetate extract of the culture filtrate of *Bacillus velezensis* strain KSAM1. GC-MS: Gas chromatography-mass spectrometry

(5.21%), Hexadecanoic acid (4.83%), 7,9-Di-tert-butyl-1-oxaspiro(4,5) deca-6,9-diene-2,8-dione (3.96%), dotriacontane (3.66%), 5-fluoro-2,2-dimethylchroman-4-one (3.37%), glycan sialylated tetraose type 2 (3.19%), pyrrolizin-1-one, 7-propyl- (2.14%), hexadecanoic acid,1-(hydroxymethyl)-1,2-ethanediyester (2.09%), docosane (2.08%), octahydrocoumarin, trans-(-)- (1.82%), oleic acid (1.72%), isochiapin B (1.70%), 2,4-Di-tert-butylphenol (1.34%), octadecanoic acid (1.14%), methanone,(1-hydroxycyclohexyl)phenyl- (0.99%), docosane, 11-decyl- (0.63%), hexadecanoic acid,2,3-dihydroxypropyl ester (0.50%), 6-ethyl-5-hydroxy-2,3,7-trimethoxy naphthoquinone (0.42%) and tetradecane, 2,6,10-trimethyl- (0.32%).

4. Discussion

The substitution of agrochemicals with PGPR applications may have far-reaching economic and environmental consequences. These may include relevant benefits such as increased yields, chemical residue reduction, no development of resistance by pests and pathogens, engagement of agricultural raw materials, and a low risk to organisms that are not the intended population. *Bacillus* is known to be able to make a variety of antimicrobial substances, including hydrolytic enzymes, volatile organic compounds (VOCs), lipopeptides, hydrogen cyanide, and siderophores. This makes it a possible biocontrol agent

for many plant pathogens. Furthermore, the capacity of endospores to develop lets them survive in hostile surroundings (Fira et al., 2018; Grahovac et al., 2023; Khan et al., 2018). As part of this work, we examined 17 different *Bacillus* isolates to see whether they could be used as bioagents against *M. phaseolina*'s mycelial progress in vitro. It was found that KSAM1 was much better than the other *Bacillus* isolates at stopping the growth of *M. phaseolina* mycelia, with a 38.6% inhibition rate. The antagonistic effects of the bioagent KSAM1 can be attributed to the fact that it secretes volatile organic chemicals and lytic enzymes that have both direct and indirect antifungal effects. The findings of (Patel et al., 2024) established that certain strains of *Bacillus* exhibited antifungal efficacy against *M. phaseolina*. These strains made *M. phaseolina* undergo morphological changes, such as a reduction in branching, a thinned mycelium, and the absence of germinating microsclerotia. It's important to remember that these results are about how well *Bacillus* strains can make VOCs, hydroperoxide, 1-methyl butyl, butanoic acid, 3-hydroxy-, methyl ester, and 2,4-azetidine-dione, 3,3-diethyl-1-methyl.

The mixing process is crucial for achieving microbial fermentations with the highest possible level of yield, and it can be accomplished through the utilization of stirring and aeration. Nevertheless, agitation at greater stirring speeds has the potential to disrupt the suspended cells in the bioreactor using the application of shave powers and the development of vortices, which may lead to a reduction in the amount

Table 2.
The list of detected compounds in the ethyl acetate extract of culture filtrate of *Bacillus velezensis* strain KSAM1.

Retention Time	Area %	Compound name	Molecular formula	Molecular weight	Compound structure
16.79	0.32	Tetradecane, 2,6,10-trimethyl-	C ₁₇ H ₃₆	240	
25.40	0.42	6-ethyl-5-hydroxy-2,3,7-trimethoxy naphthoquinone	C ₁₅ H ₁₆ O ₆	292	
31.02	0.50	Hexadecanoic acid,2,3-dihydroxypropyl ester	C ₁₉ H ₃₈ O ₄	330	
21.62	0.63	Docosane, 11-decyl-	C ₃₂ H ₆₆	450	
20.02	0.99	Methanone,(1-hydroxycyclohexyl)phenyl-	C ₁₃ H ₁₆ O ₂	204	
30.00	1.14	Octadecanoic acid	C ₁₈ H ₃₆ O ₂	284	
16.62	1.34	2,4-Di-tert-butylphenol	C ₁₄ H ₂₂ O	206	
38.38	1.70	Isochiapin B	C ₁₉ H ₂₂ O ₆	346	
29.50	1.72	Oleic acid	C ₁₈ H ₃₄ O ₂	282	
14.93	1.82	Octahydrocoumarin, trans(-)-	C ₁₀ H ₁₄ O ₂	166	
33.54	2.08	Docosane	C ₂₂ H ₄₆	310	
35.28	2.09	Hexadecanoic acid,1-(hydroxymethyl)-1,2-ethanediylester	C ₃₅ H ₆₈ O ₅	568	
15.22	2.14	Pyrrolizin-1-one, 7-propyl-	C ₁₀ H ₁₇ NO	167	
36.26	3.19	Glycan sialylated tetraose type 2	C ₃₁ H ₅₂ N ₂ O ₂₄	836	
18.76	3.37	5-fluoro-2,2-dimethylchroman-4-one	C ₁₁ H ₁₁ FO ₂	194	
41.84	3.66	Dotriacontane	C ₃₂ H ₆₆	450	
24.74	3.96	7,9-Di-tert-butyl-1-oxaspiro(4,5)deca-6,9-diene-2,8-dione	C ₁₇ H ₂₄ O ₃	276	
26.37	4.83	Hexadecanoic acid	C ₁₆ H ₃₂ O ₂	256	
25.63	5.21	Dibutyl phthalate	C ₁₆ H ₂₂ O ₄	278	
42.89	22.82	Tris(2,4-di-tert-butylphenyl) phosphate	C ₄₂ H ₆₃ O ₄ P	662	
35.77	36.07	Diisooctyl phthalate	C ₂₄ H ₃₈ O ₄	390	

of mass transfer (oxygen/substrate). It is essential to ensure that the batch operation in the bioreactor is carried out with the optimal combination of agitation and aeration capabilities (Potumarthi et al., 2007). In this investigation, two batch fermentation processes were

successfully carried out to ensure optimal agitation and aeration. Batch No. 1 was implemented with aeration at 0.5 VVM and agitation speed at 200 rpm, which gradually increased to 350 rpm in accordance with the level of DO to maintain it at a level that was greater than 20%.

In contrast, Batch No. 2 was achieved with aeration at 1 VVM and an agitation speed of two hundred rpm, which was subsequently increased to six hundred rpm. According to the findings of several studies (Cho et al., 2009; Monteiro et al., 2005; Posada-Urbe et al., 2015), accelerating the rate of cell formation can be accomplished by either raising the agitation and aeration rates or keeping the DO content at a level that is greater than 20–30%. However, higher levels of agitation can have negative effects on cells, such as the deactivation of the sporulation process, uneven cell populations, smaller cells, and even cell death (Sahoo et al., 2006).

The cell mass of *B. velezensis* strain KSAM1 grew exponentially in batch fermentation No. 1, with a specific growth rate of 0.17 h^{-1} . The maximum value of biomass was recorded at 1.65 g L^{-1} after 9 hours, whereas in batch No. 2, it achieved 3.92 g L^{-1} at 10.5 hours, with a specific growth rate of 0.08 h^{-1} , indicating a 2.38-fold increase. Our findings showed that this variation occurred in batch No. 2. Closed outcomes were obtained by (A. Soliman et al., 2022), who found that the cell mass of *B. velezensis* strain GB1 increased exponentially at a specific growth rate of 0.1 h^{-1} , resulting in a biomass of 3.8 g L^{-1} . In the current investigation, the biomass yield coefficient of the *B. velezensis* strain KSAM1 in batch No. 2 ($Y_{X/S}$, $0.7 \text{ g cell/g glucose}$) was 1.89–folds higher than the yield coefficient of biomass in batch No. 1 ($Y_{X/S}$, $0.37 \text{ g cell/g glucose}$). Fermenting the bioagent isolate B4 of *B. subtilis* in a batch fermentation process allowed (Ahmad et al., 2019) to effectively obtain a biomass yield coefficient of $0.65 \text{ g cell/g glucose}$. In a variety of growth strategies, glucose is one of the substrates used as a carbon source. It is one of the most prevalent substrates. We know that specific doses trigger substrate inhibition. According to (Ghasemi and Ahmadzadeh, 2013), it is of the utmost importance to determine the appropriate composition of the medium to encourage the growth of a specific species of bacteria. In the case of the *B. velezensis* strain KSAM1 that was under investigation, the exponential phase of the bacterial growth curve revealed that the bacteria were rapidly multiplying and consuming a considerable amount of glucose, which is a source of carbon. Batch fermentation No. 2 experienced a rapid fall in glucose concentration, whereas batch No. 1 experienced a delayed decrease. Glucose was fully consumed, which is equivalent to 0 g L^{-1} , at seven hours in batch No. 2 and eleven hours in batch No. 1. The rate of glucose intake in batch No. 2 (Q_g , $0.96 \text{ g L}^{-1} \text{ h}^{-1}$) was 4-folds higher than the consumption rate of glucose in batch No. 1 (Q_g , $0.24 \text{ g L}^{-1} \text{ h}^{-1}$). Furthermore, the biomass production rate (Q_x) in batch fermentation No. 2 was higher than that in batch No. 1, with a 2.72-fold increase.

Both batch fermentation No. 1 and batch fermentation No. 2 demonstrated a gradual decrease in DO concentration over the first 3 hours and 2 hours of the culture's growth, respectively. Additionally, the amount of dissolved oxygen reached 20% by 2.4 hours and 2 hours of the culture's growth, respectively. A gradual decrease in DO concentration was observed in batch fermentation No. 1 and No. 2 through the first three hours and two hours of the culture's growth, respectively. Furthermore, the amount of dissolved oxygen reached 20% at 2.4 and 2 hours of the culture's growth, respectively. Thus, agitation speed was increased step by step (increase by 50 rpm) to reach the supreme level of 350 rpm and 600 rpm, respectively. When the concentration of accessible oxygen is increased, more cells, spores, and beneficial metabolites are produced; however, oxygen concentration restrictions may lessen the influence of the fermentation process (Suresh et al., 2009; Wu et al., 2003). In the exponential phase, a rapid decrease in DO concentration in both fermentation processes was observed. The decrease in DO concentration in batch fermentation No. 2 was greater than the decrease in DO concentration in batch No.1. Therefore, batch No. 2 experienced a rapid increase in agitation speed from 200 rpm to 600 rpm. The DO concentration in batch No. 1 increased slowly after 7.6 hours, reaching 100% at 9 hours. On the other hand, an increase in DO concentration was observed at 10.33 hours to reach 80.2% at the end of batch fermentation No. 2. The current study shows that the bacterium *B. velezensis* strain KSAM1 needs a lot of oxygen to produce the most biomass and secondary metabolites. Before beginning the process, it is critical to cultivate the culture under optimal conditions of agitation and aeration to fulfill the culture's oxygen requirements.

Volatile organic compounds (VOCs) are organic chemical substances that readily vaporize at ambient temperatures. They consist of a varied group of lipophilic small organic compounds with high vapor

pressure and a low boiling point (Effmert et al., 2012). It has been shown in multiple studies that VOCs released by microorganisms may have positive effects on plants, such as stimulating growth, activating defense mechanisms, and reducing infection (Montejano-Ramírez et al., 2024; Philip et al., 2024; Singh et al., 2024). Some *Bacillus* species are thought to produce VOCs that protect plants from pathogenic bacteria and fungi (Poulaki and Tjamos, 2023). Some fungi, like *Colletotricum coccodes*, *Fusarium oxysporum f. sp. lycopersici*, *Botrytis cinerea*, *Rhizoctonia solani*, *Phytophthora infestans*, *Pythium ultimum*, *M. oryzae*, and *Sclerotinia sclerotiorum*, were inhibited by VOCs produced by *B. velezensis* (Lim et al., 2017). The VOCs released by *B. velezensis* VM11 caused ultrastructural damage to *S. sclerotiorum* hyphae, including to cell membranes, mitochondria, nuclei, multivesicular structures, and cytoplasm. These changes included enlarged vacuoles and disordered cytoplasmic materials, which made it hard to tell the difference between cell organelles (Massawe et al., 2018).

The present investigation used GC-MS analysis to determine which bioactive components were present in *B. velezensis* KSAM1's ethyl acetate extract. A GC-MS chromatogram of *B. velezensis* KSAM1 revealed 21 volatile organic compounds. Diisooctyl phthalate took up 36.07% of the total area. Tris (2,4-di-tert-butylphenyl)phosphate came in at 22.82%, dibutyl phthalate at 5.21%, and hexadecanoic acid at 4.83%. According to a recent proposal by (El-Enain et al., 2023), diisooctyl phthalate may have medical use in the treatment of serious bacterial infections. The most important part of the crude extract of ethyl acetate from the endophytic fungus *Paecilomyces* sp. was diisooctyl phthalate (33.77%), which was found to be harmful to *Pseudomonas aeruginosa* (Salem et al., 2022). It was reported that the antifungal activity of the ethyl acetate extract of *Penicillium* sp. against *Alternaria alternata* is attributable to diisooctyl phthalate, the extract's primary component (Lykholat et al., 2021). It facilitates wound healing and possesses the capacity to suppress microbial proliferation (Amer et al., 2019; Huang et al., 2021).

There are biological effects that can be caused by the phenolic compound known as tris (2,4-di-tert-butylphenyl) phosphate. Through its antifungal properties, the phenolic compound can inhibit the growth of *Aspergillus niger*, *P. chrysogenum*, and *F. oxysporum*. (Varsha et al., 2015). It was demonstrated that tris (2,4-di-tert-butylphenyl) phosphate has antibacterial properties against *Staphylococcus aureus*, *B. tequilensis*, *E. coli*, and *P. aeruginosa* (Abdullah et al., 2011; Murniasih et al., 2022). It was stated that phenolic chemicals can induce cytoplasmic membrane damage, enhance membrane permeability, and trigger the release of intracellular fluids, including nucleic acids, proteins, and inorganic ions (Amborabé et al., 2002). Dibutyl phthalate, an antifungal compound, is generated by *B. amyloliquefaciens* and *B. velezensis* (S. A. Soliman et al., 2022). *Bacillus* K1, an endophytic bacterium, suppressed *B. cinerea* mycelial growth and reduced grapefruit disease incidence and decay degree (Li et al., 2022). This strain's GC-MS chromatogram included primarily dibutyl phthalate. According to Li et al., 2021, dibutyl phthalate effectively prevented *C. fragariae* spore germination and hyphae formation. Dibutyl phthalate exhibits significant antifungal action against *F. oxysporum f. sp. cubense* in *Streptomyces* strain BITDG-11 (Zhang et al., 2021). In addition, actinomycete strains have expressed dibutyl phthalate as an antifungal chemical (Ahsan et al., 2017; Roy et al., 2006). Numerous therapeutic plants and metabolites from *Bacillus* spp. contain the fatty acid hexadecanoic acid (Abdelkhalek et al., 2022; Awan et al., 2023; Umaiymbigai et al., 2017; Youssef et al., 2021). According to Okwu et al. (2001), there is speculation that it possesses antifungal, hypocholesterolemic, anticancer, antibacterial, antioxidant, nematocidal, and pesticide properties. According to (El Shafay et al., 2016), the hexadecanoic acid that was produced by the *Bacillus* showed a significant amount of effectiveness in inhibiting the growth of *C. gloeosporoides*. Through its ability to attach to the active components of fungal cell walls, hexadecanoic acid can inhibit the growth of fungi. This is accomplished by forming complex molecules. Consequently, the volatile organic compounds may be responsible for the antifungal activity of *B. velezensis* strain KSAM1 against *M. phaseolina*, providing a viable explanation for this trait. Future research should focus on enhancing the understanding of the synergistic interactions among these compounds, optimizing dosages for peak efficacy, and examining practical applications in the field to validate these findings across many environmental conditions.

5. Conclusions

In terms of inhibiting mycelial growth of *M. phaseolina*, the *B. velezensis* strain KSAM1 was more effective than other isolates that achieved an inhibition percentage of 38.6%. Batch No. 2, conducted at an agitation speed ranging from 200 rpm to 600 rpm with aeration at 1 VVM, effectively enhanced the biomass of the *B. velezensis* strain KSAM1 along with the production of secondary metabolites. The highest attainable level of biomass (3.92 g L⁻¹) was obtained, and the yield coefficient was established at 0.7 g cells/g glucose. A GC-MS analysis of the strain KSAM1 culture filtrate showed that twenty-one different volatile organic compounds were found. Diisooctyl phthalate was the most important bioactive compound, making up 36.07 percent of the total area. This compound could potentially be responsible for the antagonistic effect of *B. velezensis* strain KSAM1. Without a doubt, the *B. velezensis* strain KSAM1 is a crucial biocontrol agent for managing *M. phaseolina* infections.

CRedit authorship contribution statement

Abdulaziz Al-Askar: Project administration, Funding acquisition, Supervision. **Fatimah Al-Otibi:** Visualization, Validation, Investigation. **Gaber A. Abo-Zaid:** Resources, Methodology, Formal analysis, Writing-review & editing. **Ahmed Abdelkhalik:** Methodology, Software, Writing-review & editing.

Declaration of competing interest

The authors declare that they have no known competing financial interests or personal relationships that could have appeared to influence the work reported in this paper.

Declaration of Generative AI and AI-assisted technologies in the writing process

The authors confirm that there was no use of artificial intelligence (AI)-assisted technology for assisting in the writing or editing of the manuscript and no images were manipulated using AI.

Acknowledgments

The authors extend their appreciation to the Deputyship for Research & Innovation, "Ministry of Education" in Saudi Arabia for funding this research work through the project number (IFKSUDR_F121).

References

- Abdelkhalik, A., Aseel, D.G., Király, L., Künstler, A., Moawad, H., Al-Askar, A.A., 2022. Induction of systemic resistance to tobacco mosaic virus in tomato through foliar application of bacillus amyloliquefaciens strain TBorg1 culture filtrate. *Viruses* 14, 1830. <https://doi.org/10.3390/v14081830>
- Abdelkhalik, A., Behiry, S.I., Al-Askar, A.A., 2020. Bacillus velezensis peal1 inhibits fusarium oxysporum growth and induces systemic resistance to cucumber mosaic virus. *Agronomy* 10, 1312. <https://doi.org/10.3390/agronomy10091312>
- Abdullah, A.S.H., Mirghani, M.E.S., Jamal, P., 2011. Antibacterial activity of Malaysian mango kernel. *African J. Biotechnol.* 10, 18739–18748. <https://doi.org/10.5897/AJB11.2746>
- Abed, H., Rouag, N., Mouatassem, D., Rouabhi, A., 2016. Screening for pseudomonas and bacillus antagonistic rhizobacteria strains for the biocontrol of fusarium wilt of chickpea. *Eurasian J. Soil Sci.* 5, 182–191. <https://doi.org/10.18393/ejss.2016.3.182-191>
- Ahmad, A.-G.M., Abo-Zaid, G.A., Mohamed, M.S., Elsayed, H.E., 2019. Fermentation, formulation and evaluation of PGPR Bacillus subtilis isolate as a bioagent for reducing occurrence of peanut soil-borne diseases. *J. Integr. Agric.* 18, 2080–2092. [https://doi.org/10.1016/s2095-3119\(2019\)2962578-5](https://doi.org/10.1016/s2095-3119(2019)2962578-5)
- Ahsan, T., Chen, J., Zhao, X., Irfan, M., Wu, Y., 2017. Extraction and identification of bioactive compounds (eicosane and dibutyl phthalate) produced by streptomyces strain KX852460 for the biological control of rhizoctonia solani AG-3 strain KX852461 to control target spot disease in tobacco leaf. *AMB Express* 7. <https://doi.org/10.1186/s13568-017-0351-z>
- Amorabé, B.-E., Fleurat-Lessard, P., Chollet, J.-F., Roblin, G., 2002. Antifungal effects of salicylic acid and other benzoic acid derivatives towards eutypa lata: Structure–activity relationship. *Plant Physiol. Biochem.* 40, 1051–1060. [https://doi.org/10.1016/S0981-9428\(2002\)2901470-5](https://doi.org/10.1016/S0981-9428(2002)2901470-5)

- Amer, M.S., Barakat, K.M., Hassanein, A.E.A., 2019. Phthalate derivatives from marine penicillium decumbens and its synergetic effect against sepsis bacteria. *Biointerface Res. Appl. Chem* 9, 4070–4076. <https://doi.org/10.33263/BRIAC94.070076>
- Asaka, O., Shoda, M., 1996. Biocontrol of rhizoctonia solani damping-off of tomato with Bacillus subtilis RB14. *Appl. Environ. Microbiol.* 62, 4081–4085. <https://doi.org/10.1128/aem.62.11.4081-4085.1996>
- Awam, Z.A., Shoaib, A., Schenk, P.M., Ahmad, A., Alansi, S., Paray, B.A., 2023. Antifungal potential of volatiles produced by bacillus subtilis BS-01 against alternaria solani in solanum lycopersicum. *Front. Plant Sci.* 13, 1089562. <https://doi.org/10.3389/fpls.2022.1089562>
- Caçaval, D., Galaction, A.-I., Turnea, M., 2011. Comparative analysis of oxygen transfer rate distribution in stirred bioreactor for simulated and real fermentation broths. *J. Ind. Microbiol. Biotechnol.* 38, 1449–1466. <https://doi.org/10.1007/s10295-010-0930-3>
- Cho, J.-H., Kim, Y.-B., Kim, E.-K., 2009. Optimization of culture media for bacillus species by statistical experimental design methods. *Korean J. Chem. Eng.* 26, 754–759. <https://doi.org/10.1007/s11814-009-0126-6>
- Connors, N.C., 2003. Culture medium optimization and scale-up for microbial fermentations. In: *Handbook of industrial cell culture: Mammalian, Microbial, and Plant Cells*. Springer, pp. 171–193.
- Dhingra, O.D., Sinclair, J.B., 1985. *Biology and Pathology of Macrophomina Phaseolina*. Minas Gerais: Universidade Federal de Viçosa: Imprensa Universitaria.
- Dutta, S., Bhunia, B., Raju, A., Maity, N., Dey, A., 2019. Enhanced rapamycin production through kinetic and purification studies by mutant strain of Streptomyces hygroscopicus NTG-30-27. *Chem. Pap.* 73, 2053–2063. <https://doi.org/10.1007/s11696-019-00767-0>
- Effmert, U., Kalderás, J., Warnke, R., Piechulla, B., 2012. Volatile mediated interactions between bacteria and fungi in the soil. *J. Chem. Ecol.* 38, 665–703. <https://doi.org/10.1007/s10886-012-0135-5>
- El-Enain, A., Zeatar, A., Zayed, A., Elkhawaga, M., Mahmoud, Y., 2023. Diisooctyl Phthalate as A Secondary Metabolite from Actinomycete Inhabit Animal's Dung with Promising Antimicrobial Activity. *Egypt. J. Chem.* 66, 261–277. <https://doi.org/10.21608/ejchem.2023.172600.7412>
- El Shafay, S.M., Ali, S.S., El-Sheekh, M.M., 2016. Antimicrobial activity of some seaweeds species from Red sea, against multidrug resistant bacteria. *Egypt. J. Aquat. Res.* 42, 65–74. <https://doi.org/10.1016/j.ejar.2015.11.006>
- Elsayed, E.A., Danial, E.N., Wadaan, M.A., El-Enshasy, H.A., 2019. Production of β-galactosidase in shake-flask and stirred tank bioreactor cultivations by a newly isolated bacillus licheniformis strain. *Biocatal. Agric. Biotechnol.* 20, 101231. <https://doi.org/10.1016/j.cbab.2019.101231>
- Fendrihan, S., Constantinescu, F., Siciua, O.-A., Dinu, S., 2016. Beneficial bacillus strains improve plant resistance to phytopathogens: A review. *Int. J. Environ. Agric. Biotechnol.* 1, 238512. <https://doi.org/10.22161/ijeab/1.2.7>
- Fira, D., Dimkić, I., Berić, T., Lozo, J., Stanković, S., 2018. Biological control of plant pathogens by bacillus species. *J. Biotechnol.* 285, 44–55.
- Ghasemi, S., Ahmadzadeh, M., 2013. Optimisation of a cost-effective culture medium for the large-scale production of bacillus subtilis UTB96. *Arch. Phytopathol. Plant Prot.* 46, 1552–1563.
- Grahovac, J., Pajčin, I., Vlajkov, V., 2023. Bacillus VOCs in the context of biological control. *Antibiotics* 12, 581.
- Hirpara, D.G., Gajera, H.P., Bhimani, R.D., Golakiya, B.A., 2016. The SRAP based molecular diversity related to antifungal and antioxidant bioactive constituents for biocontrol potentials of trichoderma against Sclerotium rolfsii Scc. *Curr. Genet.* 62, 619–641. <https://doi.org/10.1007/s00294-016-0567-5>
- Huang, L., Zhu, X., Zhou, S., Cheng, Z., Shi, K., Zhang, C., Shao, H., 2021. Phthalic acid esters: Natural sources and biological activities. *Toxins (Basel)*. 13, 495. <https://doi.org/10.3390/toxins13070495>
- Jahanian, A., Ramirez, J., O'Hara, I., 2024. Advancing precision fermentation: Minimizing power demand of industrial scale bioreactors through mechanistic modelling. *Comput. Chem. Eng.* 108755. <https://doi.org/10.1016/j.compchemeng.2024.108755>
- Khamis, W.M., Heflish, A.A., El-Messeiry, S., Behiry, S.I., Al-Askar, A.A., Su, Y., Abdelkhalik, A., Gaber, M.K., 2023. Swietenia mahagoni leaves extract: Antifungal, insecticidal, and phytochemical analysis. *Separations* 10, 301. <https://doi.org/10.3390/separations10050301>
- Khan, N., Martínez-Hidalgo, P., Ice, T.A., Maymon, M., Humm, E.A., Nejat, N., Sanders, E.R., Kaplan, D., Hirsch, A.M., 2018. Antifungal activity of bacillus species against fusarium and analysis of the potential mechanisms used in biocontrol. *Front. Microbiol.* 9, 2363. <https://doi.org/10.3389/fmicb.2018.02363>
- Kiesewalter, H.T., Lozano-Andrade, C.N., Wibowo, M., Strube, M.L., Maróti, G., Snyder, D., Jørgensen, T.S., Larsen, T.O., Cooper, V.S., Weber, T., 2021. Genomic and chemical diversity of bacillus subtilis secondary metabolites against plant pathogenic fungi. *Msystems* 6, 10–1128. <https://doi.org/10.1128/msystems.00770-20>
- Li, P., Feng, B., Yao, Z., Wei, B., Zhao, Y., Shi, S., 2022. Antifungal activity of endophytic bacillus K1 Against Botrytis cinerea. *Front. Microbiol.* 13, 935675.
- Li, X., Jing, T., Zhou, D., Zhang, M., Qi, D., Zang, X., Zhao, Y., Li, K., Tang, W., Chen, Y., 2021. Biocontrol efficacy and possible mechanism of Streptomyces sp. H4 against postharvest anthracnose caused by colletotrichum fragariae on strawberry fruit. *Postharvest Biol. Technol.* 175, 111401. <https://doi.org/10.1016/j.postharvbio.2020.111401>
- Lim, S.M., Yoon, M.-Y., Choi, G.J., Choi, Y.H., Jang, K.S., Shin, T.S., Park, H.W., Yu, N.H., Kim, Y.H., Kim, J.-C., 2017. Diffusible and volatile antifungal compounds produced by an antagonistic bacillus velezensis G341 against various phytopathogenic fungi. *Plant Pathol. J.* 33, 488. <https://doi.org/10.5423/ppj.oa.04.2017.0073>
- Lykholat, Y. V., Khromykh, N.O., Didur, O.O., Drehal, O.A., Sklyar, T. V., Anishchenko, A.O., 2021. Chaenomeles speciosa fruit endophytic fungi isolation and characterization of their antimicrobial activity and the secondary metabolites

- composition. Beni-Suef Univ. J. Basic Appl. Sci. 10, 1–10. <https://doi.org/10.1186/s43088-021-00171-2>
- Maral-Gül, D., Eltem, R., 2024. Evaluation of *Bacillus* isolates as a biological control agents against soilborne phytopathogenic fungi. *Int. Microbiol.* <https://doi.org/10.1007/s10123-024-00490-1>
- Marquez, N., Giachero, M.L., Declerck, S., Ducasse, D.A., 2021. *Macrophomina phaseolina*: General characteristics of pathogenicity and methods of control. *Front. Plant Sci.* 12, 634397. <https://doi.org/10.3389/fpls.2021.634397>
- Massawe, V.C., Hanif, A., Farzand, A., Mburu, D.K., Ochola, S.O., Wu, L., Tahir, H.A.S., Gu, Q., Wu, H., Gao, X., 2018. Volatile compounds of endophytic *Bacillus* spp. have biocontrol activity against sclerotinia sclerotiorum. *Phytopathology* 108, 1373–1385.
- Maurhofer, M., Keel, C., Haas, D., Défago, G., 1995. Influence of plant species on disease suppression by *Pseudomonas fluorescens* strain CHAO with enhanced antibiotic production. *Plant Pathol.* 44, 40–50.
- Meyer, W.A., Sinclair, J.B., Khare, M.N., 1974. Factors affecting charcoal rot of soybean seedlings. *Phytopathology* 64, 845–849. <https://doi.org/10.1094/phyto-64-845>
- Monteiro, S.M., Clemente, J.J., Henriques, A.O., Gomes, R.J., Carrondo, M.J., Cunha, A.E., 2005. A procedure for high-yield spore production by *Bacillus subtilis*. *Biotechnol. Prog.* 21, 1026–1031.
- Montejano-Ramírez, V., Ávila-Oviedo, J.L., Campos-Mendoza, F.J., Valencia-Cantero, E., 2024. Microbial volatile organic compounds: insights into plant defense. *Plants* 13, 2013. <https://doi.org/10.3390/plants13152013>
- Moustafa, H.E., Abd-El salam, H.E., Abo-Zaid, G.A., Serour, E.A., 2009. *As* biocontrol agent. *II. Biotechnology* 8, 35–43.
- Murniasih, T., Masteria Yunovilsa, P., Untari, F., 2022. Antibacterial activity and GC-MS based metabolite profiles of Indonesian marine *Bacillus*. *Indones J Pharm* 33, 475–483.
- Patel, J.K., Mistry, Y., Soni, R., Jha, A., 2024. Evaluation of antifungal activity of endophytic *Bacillus* spp. and identification of secondary metabolites produced against the phytopathogenic fungi. *Curr. Microbiol.* 81, 128. <https://doi.org/10.1007/s00284-024-03652-6>
- Philip, B., Behiry, S.I., Salem, M.Z.M., Amer, M.A., El-Samra, I.A., Abdelkhalek, A., Heflish, A., 2024. *Trichoderma afroharzianum* TRI07 metabolites inhibit *Alternaria alternata* growth and induce tomato defense-related enzymes. *Sci. Rep.* 14, 1874. <https://doi.org/10.1038/s41598-024-52301-2>
- Posada-Urbe, L.F., Romero-Tabarez, M., Villegas-Escobar, V., 2015. Effect of medium components and culture conditions in *Bacillus subtilis* EA-CB0575 spore production. *Bioprocess Biosyst. Eng.* 38, 1879–1888. <https://doi.org/10.1007/s00449-015-1428-1>
- Potumarthi, R., Ch, S., Jetty, A., 2007. Alkaline protease production by submerged fermentation in stirred tank reactor using *Bacillus licheniformis* NCIM-2042: effect of aeration and agitation regimes. *Biochem. Eng. J.* 34, 185–192. <https://doi.org/10.1016/j.bej.2006.12.003>
- Poulaki, E.G., Tjamos, S.E., 2023. *Bacillus* species: Factories of plant protective volatile organic compounds. *J. Appl. Microbiol.* 134, 1xad037. <https://doi.org/10.1093/jambio/1xad037>
- Rangel-Montoya, E.A., Delgado-Ramírez, C.S., Sepulveda, E., Hernández-Martínez, R., 2022. Biocontrol of *Macrophomina phaseolina* using *Bacillus amyloliquefaciens* strains in cowpea (*Vigna unguiculata* L.). *Agronomy* 12, 676.
- Roy, R.N., Laskar, S., Sen, S.K., 2006. Dibutyl phthalate, the bioactive compound produced by *Streptomyces albidoflavus* 321.2. *Microbiol. Res.* 161, 121–126. <https://doi.org/10.1016/j.micres.2005.06.007>
- Sabaté, D.C., Petroselli, G., Erra-Balsells, R., Audisio, M.C., Brandan, C.P., 2020. Beneficial effect of *Bacillus* sp. P12 on soil biological activities and pathogen control in common bean. *Biol. Control* 141, 104131. <https://doi.org/10.1016/j.biocontrol.2019.104131>
- Sahoo, S., Rao, K.K., Suraiskumar, G.K., 2006. Reactive oxygen species induced by shear stress mediate cell death in *Bacillus subtilis*. *Biotechnol. Bioeng.* 94, 118–127.
- Salahlou, R., Safaie, N., Shams-Bakhsh, M., 2016. Genetic diversity of *Macrophomina phaseolina* populations, the causal agent of sesame charcoal rot using inter-simple sequence repeat markers. *J. Agric. Sci. Technol.* 18, 277–287.
- Salem, S.H., El-Maraghy, S.S., Abdel-Mallek, A.Y., Abdel-Rahman, M.A.A., Hassanein, E.H.M., Al-Bedak, O.A., El-Aziz, F.E.-Z.A.A., 2022. The antimicrobial, antibiofilm, and wound healing properties of ethyl acetate crude extract of an endophytic fungus *Paecilomyces* sp. (AUMC 15510) in earthworm model. *Sci. Rep.* 12, 19239.
- Sassenrath, G., Waite, N., Hsiao, C.-J., Little, C.R., 2024. Brassica juncea pre-season cover crops reduce soybean root colonization by *Macrophomina phaseolina*, the fungus causing charcoal rot. *Plant Heal. Prog.*
- Sharma, D., Pramanik, A., Agrawal, P.K., 2016. Evaluation of bioactive secondary metabolites from endophytic fungus *Pestalotiopsis neglecta* BAB-5510 isolated from leaves of *Cupressus torulosa* D. Don. *3 Biotech* 6, 210.
- Singh, P., Singh, J., Ray, S., Vaishnav, A., Jha, P., Singh, R.K., Singh, H.B., 2024. Microbial volatiles (mVOCs) induce tomato plant growth and disease resistance against wilt pathogen *Fusarium oxysporum* f. sp. *lycopersici*. *J. Plant Growth Regul.* 43, 3105–3118.
- Soliman, A., Matar, S., Abo-Zaid, G., 2022. Production of *Bacillus velezensis* strain GB1 as a biocontrol agent and its impact on *Bemisia tabaci* by inducing systemic resistance in a squash plant. *Horticulturae* 8, 511.
- Soliman, S.A., Khaleil, M.M., Metwally, R.A., 2022. Evaluation of the antifungal activity of *Bacillus amyloliquefaciens* and *B. velezensis* and characterization of the bioactive secondary metabolites produced against plant pathogenic fungi. *Biology (Basel)*. 11, 1390.
- Suresh, S., Srivastava, V.C., Mishra, I.M., 2009. Techniques for oxygen transfer measurement in bioreactors: A review. *J. Chem. Technol. Biotechnol. Int. Res. Process. Environ. Clean Technol.* 84, 1091–1103. <https://doi.org/10.1002/jctb.2154>
- Torres, M.J., Brandan, C.P., Sabaté, D.C., Petroselli, G., Erra-Balsells, R., Audisio, M.C., 2017. Biological activity of the lipopeptide-producing *Bacillus amyloliquefaciens* PGPBacCA1 on common bean *Phaseolus vulgaris* L. pathogens. *Biol. Control* 105, 93–99. <https://doi.org/10.1016/j.biocontrol.2016.12.001>
- Umairambigai, D., Saravanakumar, K., Raj, A.G., 2017. Phytochemical profile and antifungal activity of leaves methanol extract from the *Psydrax dicoccos* (Gaertn) teys. & binn. rubiaceae family. *Int J Pharma Phytochem Ethnomed* 7, 53–56.
- Van Dam-Mieras, M.C.E., Jeu, W.H., Vries, J., Currell, B.R., James, J.W., Leach, C.K., Patmore, R.A., 1992. Techniques used in bioproduct analysis.
- Varsha, K.K., Devendra, L., Shilpa, G., Priya, S., Pandey, A., Nampoothiri, K.M., 2015. 2, 4-Di-tert-butyl phenol as the antifungal, antioxidant bioactive purified from a newly isolated *Lactococcus* sp. *Int. J. Food Microbiol.* 211, 44–50.
- Wu, Z., Du, G., Chen, J., 2003. Effects of dissolved oxygen concentration and DO-stat feeding strategy on CoQ 10 production with *Rhizobium radiobacter*. *World J. Microbiol. Biotechnol.* 19, 925–928.
- Yassin, Y., Aseel, D., Khalil, A., Abdel-Megeed, A., Al-Askar, A., Elbeaino, T., Moawad, H., Behiry, S., Abdelkhalek, A., 2024. Foliar application of *Rhizobium leguminosarum* bv. *viciae* strain 33504-Borg201 promotes faba bean growth and enhances systemic resistance against bean yellow mosaic virus infection. *Curr. Microbiol.* 81, 220. <https://doi.org/10.1007/s00284-024-03733-6>
- Youssef, N.H., Qari, S.H., Behiry, S.I., Dessoky, E.S., El-Hallous, E.I., Elshaer, M.M., Kordy, A., Maresca, V., Abdelkhalek, A., Heflish, A.A., 2021. Antimycotoxic activity of beetroot extracts against *Alternaria alternata* mycotoxins on potato crop. *Appl. Sci.* 11, 4239. <https://doi.org/10.3390/app11094239>
- Zhang, L., Zhang, H., Huang, Y., Peng, J., Xie, J., Wang, W., 2021. Isolation and evaluation of rhizosphere actinomycetes with potential application for biocontrolling *Fusarium wilt* of banana caused by *Fusarium oxysporum* f. sp. *cubense* tropical race 4. *Front. Microbiol.* 12, 763038. <https://doi.org/10.3389/fmicb.2021.763038>
- Zhou, Y., Han, L.-R., He, H.-W., Sang, B., Yu, D.-L., Feng, J.-T., Zhang, X., 2018. Effects of agitation, aeration and temperature on production of a novel glycoprotein GP-1 by *Streptomyces kanasensis* ZX01 and scale-up based on volumetric oxygen transfer coefficient. *Molecules* 23, 125. <https://doi.org/10.3390/molecules23010125>